ANALYSIS OF SCALAR DISSIPATION RATE AND TURBULENT TRANSPORT IN LES OF PREMIXED TURBULENT COMBUSTION

Pascale Domingo, Luc Vervisch, Sandra Payet, Raphael Hauguel
LMFN - UMR6614 - CORIA,
INSA de Rouen - Campus du Madrillet, BP8
F-76801 Saint-Etienne-du-Rouvray Cedex, France
domingo@coria.fr, vervisch@coria.fr, payet@coria.fr

ABSTRACT

Using a priori filtering of DNS of a premixed turbulent V-shape flame, closures for the filtered scalar dissipation rate and turbulent transport are discussed. Then, a novel subgrid scale closure for Large Eddy Simulation of premixed combustion is proposed. This approach combines a presumed Probability Density Function, accounting for the subgrid scale characteristic flame length scale, with a flame tabulated chemistry approach (FPI). The ORACLES experiment is used as a first validation test case.

INTRODUCTION

Turbulent combustion is inherently an unsteady process and the objective of Large Eddy Simulation (LES) is to capture the behavior of most of the large scales of the flow. A filtering operation is applied to any instantaneous signal $c(\underline{x},t)$, such that:

$$\overline{c}(\underline{x},t) = \int_{-\infty}^{+\infty} c(\underline{x}',t)\mathcal{G}_\Delta(\underline{x}-\underline{x}')d\underline{x}' \qquad (1)$$

where $\mathcal{G}_\Delta(\underline{x}-\underline{x}')$ is a spatial filter of characteristic size Δ. Mass weighted filtering may be deduced from Eq. 1, $\widetilde{c} = \overline{\rho c}/\overline{c}$. Spatial filtering introduces SubGrid Scale (SGS) fluctuations that can be calibrated from the SGS energy, or SGS variance:

$$\widetilde{c}_v = \widetilde{cc} - \widetilde{c}\,\widetilde{c} \qquad (2)$$

When the filter $\mathcal{G}_\Delta$ is applied to a premixed turbulent flame, SGS fluctuations result from two combined effects: (a) The thickening of the thin flame front over the coarse LES grid and (b) The wrinkling of the flame within the subgrid that results from interaction with subgrid vortices. (a) and (b) are intricately related and cannot a priori be distinguished when performing LES of turbulent flames.

A description of the global SGS behavior of the flame is achieved when the filtered progress variable $\widetilde{c}$, its variance $\widetilde{c}_v$ and eventually its corresponding scalar dissipation rate $\overline{\rho}\widetilde{\chi}_c = \overline{\rho D|\nabla c|^2}$ are known, those quantities being basic ingredient of presumed probability density function or flamelet modeling (Bray, 1996). In addition, SGS turbulent transport $\overline{\tau}_c = \overline{\rho \mathbf{u} c} - \overline{\rho}\widetilde{\mathbf{u}}\widetilde{c}$ also needs closure.

In a first stage, to address these topics, Direct Numerical Simulation (DNS) of a premixed V-Flame is analysed. The database is filtered to collect informations and evaluate SGS modeling for the subgrid scalar dissipation rate and $\overline{\tau}_c$. Then, the One Rig for Accurate Comparisons with Large-Eddy Simulations (ORACLES) experiment (Nguyen and Bruel, 2003a; Nguyen and Bruel, 2003b), is simulated. The chemical source terms are closed with a new form of presumed PDF that allows for including detailled chemistry from a FPI flame generated tabulation (Gicquel et al., 2000). The PDF includes a SGS flame length scale deduced from flame surface density.

V-FLAME DNS ANALYSIS

DNS database

The premixed turbulent V-Flame DNS database first discussed at TSFP-3 (Vervisch et al., 2004) (figs. 1-2) is used for the first part of this work. The fully compressible Navier-Stokes equations are solved and the flame is described using FPI tabulated chemistry of a stoichiometric methane-air mixture using the GRI mechanism (Bowman et al., 1997). The turbulence entering the computational domain is generated with a spectral solver coupled to the compressible solution through the inlet boundary conditions. This requires a careful treatment of acoustic waves and turbulence forcing that is detailed elsewhere (Guichard et al., 2004). The compressible solver is based on the sixth order PADE (Lele, 1992) scheme for the spatial derivatives and a third order Runge-Kutta scheme for time integration.

Laminar reference flame quantities combined with turbulent scales are useful to calibrate premixed combustion DNS. In premixed flames, a possible reference length is the laminar flame thickness $\delta_L = (D/S_L)$, where D is a representative diffusion coefficient and S_L the stoichiometric laminar flame speed. δ_L and S_L are computed from a reference planar, laminar and unstrained premixed flame. Three simulations have been performed varying the level of turbulence. The inflow mean velocity is $10S_L$. The less turbulent flame, denoted case (i), features a ratio between the velocity fluctuations (at the inlet) and S_L that is of the order of 1.25. This ratio is of the order of 2.5 in the second flame, denoted case (ii), and of the order of 3.75 in the third flame, denoted case (iii). The Karlovitz number is 0.43 in case (i), 1.21 in case (ii) and 2.2 in case (iii). The ratio between the integral length scale and the flame thickness is ten time smaller than in representative experiments of V-Flame (fig. 1(a)). The simulations are

two-dimensional, the mesh of the zone upstream of the flame where the forced turbulence is computed is 512×512 (case (i)) and 512×1024 (cases (ii) and (iii)) (spectral), while the flame requires a 1024x1024 grid for case (i) and 1024x2048 in case (ii) and (iii) (finite difference). Two-dimensionality is an oversimplification. Nevertheless, it was shown that most properties of premixed flame turbulence interaction are found in two-dimensional DNS, as a result of the typical behavior of premixed flame surfaces when they interact with vorticity (Poinsot and Veynante, 2005).

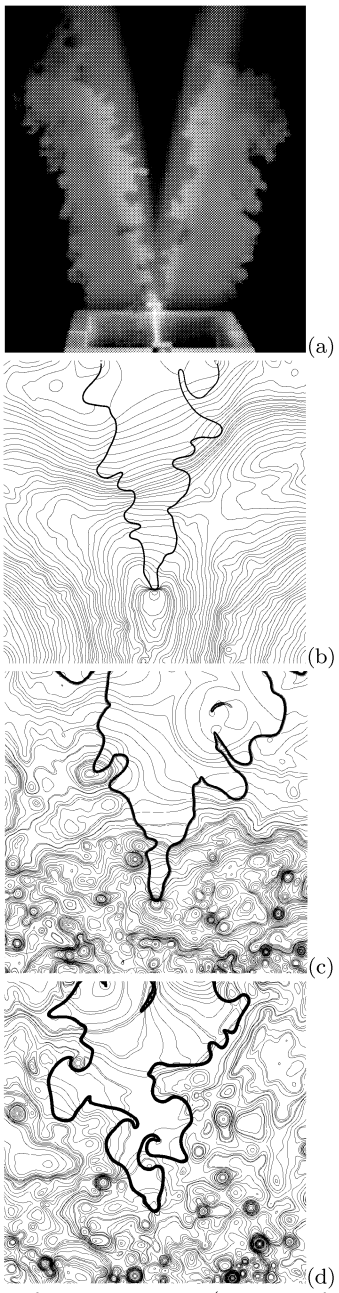

Figure 1: (a): V-Flame experiment (Renou and Boukhalfa, 2003). (b): DNS Case (i). (c): DNS Case (ii). (d): DNC case (iii). Pressure field (line) and reaction rate (bold). The flow goes from bottom to top.

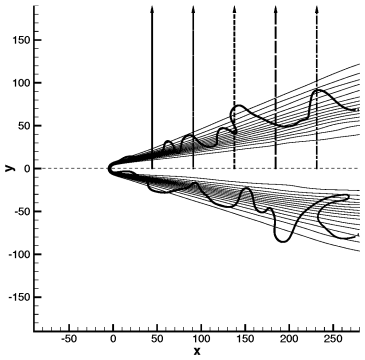

Figure 2: Averaged field of the progress variable (RANS), $\langle c \rangle$. Case (i). Thin lines: 14 levels between $\langle c \rangle = 0.1$ and $\langle c \rangle = 0.98$. Thick line: Instantaneous burning rate. The locations where transverse profiles are extracted are shown. Same locations are used in cases (ii) and (iii). The flow goes from left to right, x: Horizontal, y: Vertical.

SGS scalar dissipation rate

The RANS scalar dissipation rate of the progress variable has been previously analyzed with this DNS database and a model constructed from the decomposition of the scalar dissipation rate into a turbulent flame characteristic mixing speed and a flame wrinkling length (Vervisch et al., 2004). Using the same type of type of decomposition, a closure is now tested for the filtered scalar dissipation rate appearing in Large Eddy Simulation context.

Introducing a surface filter $\langle a \rangle_s = \overline{a|\nabla c|}/\overline{|\nabla c|}$, one may write:

$$\overline{\rho}\widetilde{\chi_c} = \overline{\rho D|\nabla c|^2} = \langle \rho D|\nabla c| \rangle_s \, \overline{|\nabla c|} \qquad (3)$$

The filtered speed of mixing $\langle \rho D|\nabla c| \rangle_s$ can be approximated by its value in a filtered one-dimensional unstrained premixed flamelet. Then, $\overline{|\nabla c|}$ represents the subgrid scale flame surface density and contains information on the subgrid flame wrinkling. A closure of this term may be written (Boger, 2000): $\overline{|\nabla c|} = K\overline{c}(1-\overline{c})/\Delta$, where K is a modeling constant of the order of unity and Δ the filter size.

The comparison between the filtered DNS and the closure Eq. (3) of the scalar dissipation rate is presented in fig. 3. The value of the subgrid scale flame surface density issued from DNS is employed here, while $< \rho D|\nabla c| >_s$ is tabulated from the FPI unstrained premixed flamelet. The modeled expression of the dissipation rate gives an interesting approximation of the exact one obtained after filtering the DNS.

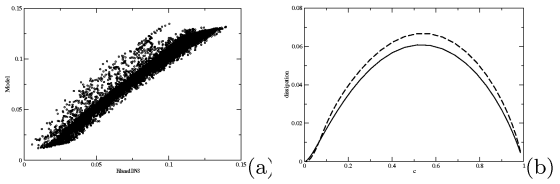

Figure 3: Filtered scalar dissipation rate: comparison between closure Eq. (3) and filtered DNS for $\Delta/\delta_{fl} = 12$. (a): Scatter plot, Case (i). (b): Cut at position x = 140. Line: filtered DNS. Dashed line: model. case (iii).

Turbulent transport in V-Flame

Turbulent transport in premixed flames has been the subject of many studies. The unresolved fluxes of the progress variable, $\overline{\tau}_{i_c} = \overline{\rho u_i c} - \overline{\rho}\widetilde{u}_i\widetilde{c}$ appear in the balance equation for $\tilde{c}$ and needs closure. In RANS, it was found that both gradient and counter gradient transports occur, depending on various flame control parameters, as the level of heat release or mean pressure gradients (see the work of Veynante et al for details (Veynante et al., 1997; Veynante and Poinsot, 1997)).

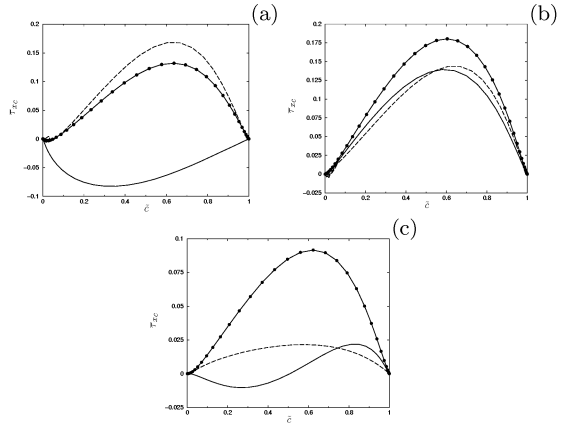

Figure 4: Transverse profiles of the streamwise SGS flux, $\overline{\rho uc} - \overline{\rho}\widetilde{u}\widetilde{c}$, versus Favre filtered progress variable (a): x= 47.7. (b): x = 95.8. (c): x = 240. Lines with symbols: Case (i). Lines: Case (ii). Dashed lines: Case (iii).

SGS turbulent fluxes are obtained by filtering DNS. The results presented are obtained with a filter size $\Delta/\delta_L = 12$. Smaller filter sizes have also been used without affecting the sign of the fluxes. As expected, as the filter size is decreased the intensity of the SGS turbulent fluxes also decreases. The SGS streamwise flux $\overline{\tau}_{x_c}$ is presented in Fig. 4. The flames with weak and strong turbulence (case (i) and case (iii)) feature counter-gradient diffusion, while case (ii) displays both SGS gradient and counter-gradient diffusion. Contrary to what is observed with RANS averaging, the sign of the subgrid flux does not seem to be clearly related to the local intensity of the turbulence. The ratio $\overline{\tau}_{x_c}/\overline{\rho uc}$ stays below 4%, indicating that the contribution of the SGS turbulent flux stays quite small (u is the streamwise (x) component of the velocity). The previous result is similar to what has been obtained by Boger (Boger, 2000) from similar a-priori filtering of planar premixed flames DNS. The turbulent flux in the transverse direction, $\overline{\tau}_{y_c}$, is given in Fig. 5. The fluxes are found to be counter-gradient for all positions and flames. Here the ratio $\overline{\tau}_{y_c}/\overline{\rho vc}$ is quite large (up to 100%), (v is the spanwise (y) component of the velocity). Nevertheless, this transverse flux stays small compared to other terms entering the balance equation for $\tilde{c}$ (not shown).

The weak contribution of the LES SGS fluxes measured in those DNS, specifically when compared to the RANS ones, suggests that the modeling of turbulent transport in premixed flames may be easier to handle with LES than with RANS. Even though this preliminary conclusion has to be considered with great care since the range of scales present in the DNS is quite limited, this is an encouraging results for LES of premixed turbulent combustion.

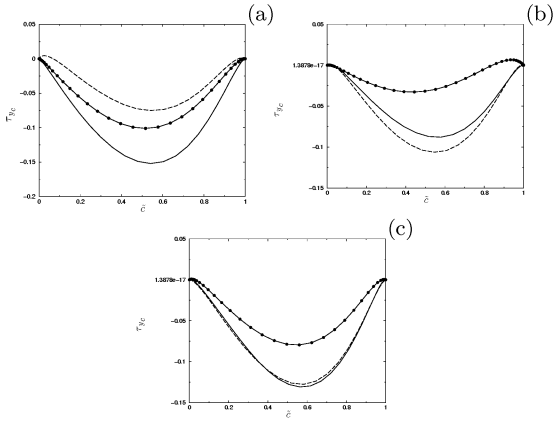

Figure 5: Transverse profiles of the spanwise SGS flux, $\overline{\rho vc} - \overline{\rho}\widetilde{v}\widetilde{c}$, versus Favre filtered progress variable. (a): x= 47.7. (b): x = 95.8. (c): x = 240. Lines with symbols: Case (i). Lines: Case (ii). Dashed lines: Case (iii).

LES OF PREMIXED COMBUSTION WITH TABULATED CHEMISTRY

Σ-PDF SGS closure

Tabulation of chemistry from laminar premixed flames, as FPI or FGM methods (Fiorina et al., 2005; van Oijen et al., 2001) are attractive since they allow for introducing effects of detailed chemistry with a very low number of transported variables. This concept was first introduced for RANS by Bradley and coworkers (Bradley et al., 1988; Bradley et al., 1998). One open question left is the impact of unsteadiness and the possible use of this approach as a SGS description of chemistry for LES, this is the main objective of this section. Propane/Air combustion is considered at equivalence ratio 0.75. The GRI mechanism (Bowman et al., 1997) is used with the PREMIX (Kee et al., 1992) complex chemistry flame solver for simulating the FPI reference flame.

As it was done for DNS above, a reaction progress variable is defined after normalising $Y_c = Y_{CO} + Y_{CO_2}$ with its equilibrium value measured in fully burnt products, $c = Y_c/Y_c^{Eq}$. The source of $\widetilde{c}$ and of any species mass fraction may be obtained from the FPI table as:

$$\widetilde{\Psi}(\underline{x},t) = \int_0^1 \Psi^{FPI}(c^*)\widetilde{P}(c^*;\underline{x},t)dc^* \tag{4}$$

Where, $\widetilde{P}(c^*;\underline{x},t)$ is a subgrid scale PDF (Gao and E.O'Brien, 1993; Cook et al., 1997; Jaberi et al., 1999). Beta function based on the knowledge of the filtered value of the progress variable ($\tilde{c}$) and its subgrid variance ($\tilde{c}_v$) are usually used to presume SGS PDFs. But, this does not include any information on the inner flame structure and may prove to be inadequate when SGS fluctuations are high (very weak resolution of the flame on the mesh). To account for the characteristic length associated to the reaction zone, the shape of the presumed PDF may be obtained from the flame surface density Σ (Vervisch et al., 2004):

$$\widetilde{P}(c^*;\underline{x},t) = \frac{\Sigma(c^*;\underline{x},t)}{\left(\overline{|\nabla c||c^*}\right)} \tag{5}$$

Because the flame is locally thin, it is assumed that within the range $0 < c^* < 1$, the iso-surfaces stay mostly parallel to each other, a behaviour confirmed by DNS (Poinsot and Veynante, 2005). Accordingly, $\Sigma(c^*, \underline{x}, t)$ weakly varies in the internal part of the diffusive-reactive layer. However, it strongly depends on Δ/δ_{fl}. The internal part of the PDF ($0 < c^* < 1$) may then be approximated as:

$$P(c^*; \underline{x}, t) = \frac{\sigma(\underline{x}, t)}{\overline{G}_\Delta(c^*)} H(c^*)H(1-c^*) \tag{6}$$

$\sigma(\underline{x}, t)$ is a quantity to be determined. H is the Heaviside function and $\overline{G}_\Delta(c^*)$ is the gradient distribution measured from the FPI reference planar and unstrained flame that has been filtered at the level Δ:

$$\overline{G}_\Delta(c(x)) = \int_{-\infty}^{+\infty} |\nabla c|^{FPI} \mathcal{G}_\Delta(x - x')dx' \tag{7}$$

The role of Σ within the Σ-PDF closure is to introduce a measure of the characteristic flame length that interacts with turbulence within the subgrid, and that is viewed on the resolved field at the given scale Δ. The distribution of the gradient of a progress variable within a reference filtered flamelet is combined with Σ to determine the internal part of a double delta PDF, then approximating SGS flame intermitency. This PDF is particularly useful when the amount of SGS energy is large and is organised as:

$$\begin{aligned} \widetilde{P}(c^*; \underline{x}, t) &= \alpha(\underline{x}, t)\delta(c^*) + \beta(\underline{x}, t)\delta(1-c^*) \\ &+ \frac{\sigma(\underline{x}, t)}{\overline{G}_\Delta(c^*)} H(c^*)H(1-c^*) \end{aligned} \tag{8}$$

The presumed PDF relies on three parameters, α, β and σ that need to be determined from mass conservation, and first ($\widetilde{c}$) and second ($\widetilde{c_v}$) moment of the SGS PDF. Filtered quantities are tabulated after combining the PDF of the progress variable with the FPI table (Eq. 4). The use of this table avoids any PDF calculation during the simulations, keeping cpu time to a reasonably low level. Balance equations are solved to estimate the filtered values of the progress variable and its SGS variance. For various LES practical reasons, the departure between the variance and its local theoretical maximum level, $\tilde{\varphi}_c$, is transported instead of the variance itself. The relation between $\tilde{c}_v$ and $\tilde{\varphi}_c$ is:

$$\widetilde{c}_v = \widetilde{c}\,\widetilde{c} - \widetilde{c}\widetilde{c} = \widetilde{c}(1-\widetilde{c}) - \widetilde{\varphi}_c \tag{9}$$

The closed balance equations to be solved to determined the presumed pdf may be written:

$$\frac{\partial \overline{\rho}\widetilde{c}}{\partial t} + \nabla \cdot (\overline{\rho}\widetilde{\mathbf{u}}\widetilde{c}) = \nabla \cdot \left(\overline{\rho}(D + (\nu_T/Sc_T))\nabla\widetilde{c}\right) + \overline{\rho}\widetilde{\omega}_c \tag{10}$$

$$\begin{aligned} \frac{\partial \overline{\rho}\widetilde{\varphi}_c}{\partial t} &+ \nabla \cdot (\overline{\rho}\widetilde{\mathbf{u}}\widetilde{\varphi}_c) = \nabla \cdot \left(\overline{\rho}(D + (\nu_T/Sc_T))\nabla\widetilde{\varphi}_c\right) \\ &+ 2\overline{\rho D|\nabla c|^2} \\ &+ \overline{\rho}\left(\widetilde{\omega}_c - 2\widetilde{\omega_c c}\right) \end{aligned} \tag{11}$$

The dissipation term, $\overline{\rho D|\nabla c|^2}$, is a source in Eq. 11 and is closed with the novel closure given in Eq. 3. As mentioned in the previous section, the contribution of the nonresolved turbulent fluxes is weak. Then, a simple gradient assumption is retained.

LES of the ORACLES experiment

The ORACLES experiment was specifically designed for LES validation by Nguyen and Bruel (Nguyen and Bruel, 2003a; Nguyen and Bruel, 2003b). It consists of two channels of fully premixed mixtures separated by a splitter plate and exposed to a sudden expansion (Fig. 6).

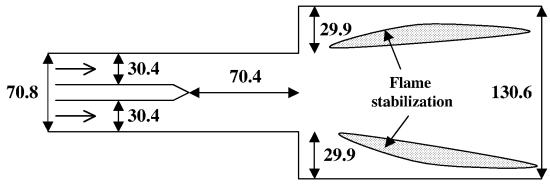

Figure 6: Sketch of the ORACLES experiment (Nguyen and Bruel, 2003a; Nguyen and Bruel, 2003b). Length are in mm.

The channels are 3 meters long to obtain a fully developed turbulent channel flow. The combustion chamber is located after the sudden expansion and is 2 meter long with insulated walls. The outlet was carefully set to monitor the outflow rate of the rig (3.5 m^3/s). The bulk velocity is of the order of $U_d = 11.0$ m/s. The Reynolds number estimated from U_d, the height of the inlet channel $H = 30.4$ mm and the viscosity of fresh mixture at the reference temperature $T_0 = 276K$, is of the order of 25 000. In the transverse direction, the depth of the channel is 150.5 mm. The flame is stabilised in the shear layers that develop after the sudden expansion and transverse distributions of mean velocity measurements are available at various streamwise locations. The reported simulations focusses on the case where the equivalence ratio is $\Phi = 0.75$ in both streams. Experiments are available for both non reacting and combusting flows. Previous LES of this experiment under other conditions of equivalence ratio have already been performed with success using a different SGS modeling strategy (Pitsch and de Lageneste, 2002).

The fully compressible set of Navier-Stokes equations together with the balance equations for $\widetilde{c}$ and $\widetilde{\varphi}_v$ (Eq. 10) are solved using a fourth order finite volume skew-symmetric-like scheme proposed by Ducros et al. (Ducros et al., 2000) for the spatial derivatives. This scheme was specifically developed and tested for LES, it is combined with a second order Runge Kutta explicit time stepping. Because the equations are solved in their fully compressible form, the time step limitation includes acoustic waves and Navier-Stokes Characteristic Boundary Conditions are retained (Poinsot and Lele, 1992). The various parameters of SGS dynamic modeling closing the Navier-Stokes equations are evaluated from the Lagrangian dynamic procedure (Meneveau et al., 1996).

The unsteady behavior of the ducted flame was carefully identified and calibrated by time series measurements (Nguyen and Bruel, 2003a; Nguyen and Bruel, 2003b). For the case studied ($\Phi = 0.75$), a specific acoustic mode with large scale fluctuations at a characteristic frequency of the order of 50 Hz was found. The natural reproduction of this acoustic mode with LES would need the simulation of the full length of the rig, or the use of a specific methodology for capturing the

acoustic properties of combustion chambers with LES, as recently discussed by Roux et al (Roux et al., 2005). This is not the objective of this first validation of Σ-PDF SGS modeling. To avoid simulating the full system, preliminary simulations of the channel flows, upstream of the main combustion chamber, were performed to generate proper inlet conditions, which are then acoustically perturbed according to the spectrum experimentally measured in the inlet plane of the combustion chamber (Nguyen and Bruel, 2003a; Nguyen and Bruel, 2003b), right after the splitter plate. Following this procedure, only 45 cm long of the facility is computed, just after the sudden expansion with a spanwise length of 7 cm. The three-dimensional non-uniform grid is composed of 128×96×32 nodes. In the region where the flame develops the grid is such that $\Delta/\delta_{fl} \approx 20$ and this value is retained in the Σ-PDF.

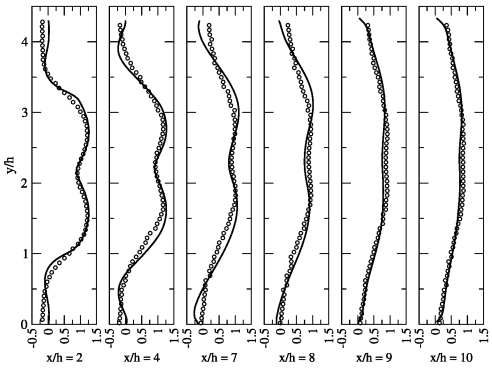

Figure 7: Non reacting flow: Transverse distribution of time averaged streamwise velocity. Symbol: Experiment. Line: LES .

The non-reacting flow is simulated at first to estimate the prediction capabilities of the LES procedure chosen. Acoustic perturbation are not added in that case since the 50 Hz oscillation is not observed without combustion. The cold flow is found to be non-symmetric in the transverse direction, which is a characteristic of double-step expansion flows when the ratio h/W is greater than 0.5, where $h = 29.9$ mm is the step height and $W = 35.4$ mm is the half width of the inlet channel (Abbott and Kline, 1962). Figure 7 displays the distribution of time averaged filtered streamwise velocity at several stations along the channel. The velocity is made non-dimensional by the bulk velocity U_d. The computed velocity compares well with the experimental one and the slight non-symmetrical character of the flow is captured.

When the flow is reacting, the symmetry of the flow is recovered. Figures 8 and 9 show distributions of time average filtered streamwise, transverse, and RMS velocity. Most of the reacting flow structure is well reproduced, especially the streamwise velocity that is correctly captured. The level of RMS velocity is also in agreement with experiment. This preliminary test is thus encouraging.

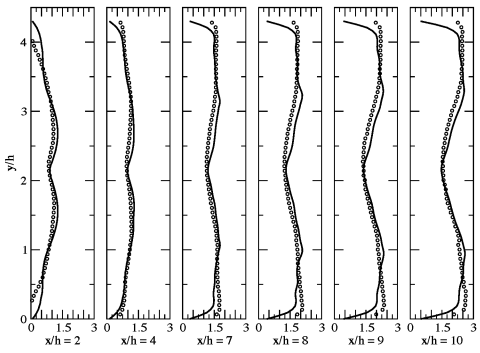

Figure 8: Reacting flow: Transverse distribution of time averaged streamwise velocity. Symbol: ORACLES experiment. Line: LES.

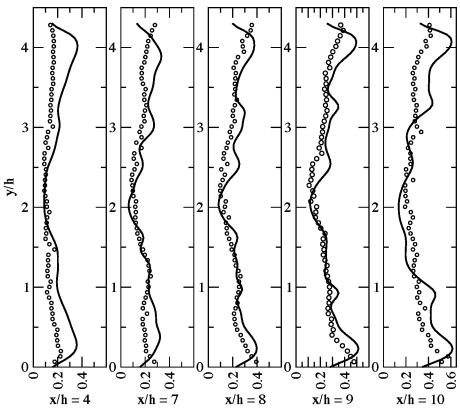

Figure 9: Reacting flow: Transverse distribution of time averaged RMS velocity. Symbol: Experiment. Line: LES.

REFERENCES

Abbott, D. E. and Kline, S. J. (1962). Experimental investigation of subsonic turbulent flow over single and double backward facing steps. *J. Basic Engineering*, pages 317–325.

Boger, M. (2000). *Modélisation de sous-maille pour la simulation aux grandes échelles de la combustion turbulente prémélangée*. PhD thesis, Ecole Centrale Paris (France).

Bowman, C. T., Hanson, R. K., Gardiner, W. C., Lissianski, V., Frenklach, M., Goldenberg, M., Smith, G. P., Crosley, D. R., and Golden, D. M. (1997). An optimized detailed chemical reaction mechanism for methane combustion and no formation and reburning. Technical report, Gas Research Institute, Chicago, IL. Report No. GRI-97/0020.

Bradley, D., Gaskell, P. H., and Gu, X. J. (1998). The mathematical modeling of liftoff and blowoff of turbulent non-premixed methane jet flames at high strain rate. In *Twenty-Seventh Symposium (Int.) Symposium on combustion*, pages 1199–1206.

Bradley, D., Kwa, L. K., Lau, A. K. C., and Missaghi, M. (1988). laminar flamelet modeling of recirculating premixed methane and propane-air combustion. *Combust. Flame*, 71:109–122.

Bray, K. N. C. (1996). The challenge of turbulent combustion. *Proc. Combust. Inst.*, 26:1–26.

Cook, A. W., Riley, J. J., and Kosály, G. (1997). A laminar flamelet approach to subgrid-scale chemistry in turbulent flows. *Combust. Flame*, 109(3):332–341.

Domingo, P., Payet, S., Hauguel, R., and Vervisch, L. (2005). Dns of premixed turbulent v-flame and les of a ducted-flame using a σ-pdf subgrid scale closure. *Combust. Flame*, submitted.

Ducros, F., Laporte, F., Soulères, T., Guinot, V., Moinat, P., and Caruelle, B. (2000). High-order fluxes for conservative skew-symmetric-like schemes in structured meshes: application to compressible flows. *J. Comput. Phys.*, 161:114–139.

Fiorina, B., Gicquel, O., Vervisch, L., and Darabiha, N. (2005). Premixed turbulent combustion modeling using tabulated detailed chemistry and pdf. *Proc. Combust. Inst*, 30.

Gao, F. and E.O'Brien, E. (1993). A large-eddy simulation scheme for turbulent reacting flows. *Phys. Fluids*, 5(6):1282–1284.

Gicquel, O., Darabiha, N., and Thevenin, D. (2000). Laminar premixed hydrogen / air counterflow flame simulations using flame prolongation of ildm with differential diffusion. *Proc. Comb. Inst.*, 28:1901–1908.

Guichard, L., Réveillon, J., and Hauguel, R. (2004). Direct numerical simulation of statistically stationary one- and two-phase turbulent combustion: a turbulent injection procedure. *Flow Turbulence and Combustion*, In press.

Jaberi, F. A., Colucci, P. J., James, S., Givi, P., and Pope, S. B. (1999). Filtered mass density function for large-eddy simulation of turbulent reacting flows. *J. Fluid Mech.*, 401:85–121.

Kee, R. J., Grcar, J. F., Smooke, M. D., and Miller, J. A. (1992). A fortran program for modeling steady laminar one-dimensional premixed flames. Technical report, Sandia National Laboratories.

Lele, S. K. (1992). Compact finite difference schemes with spectral like resolution. *J. Comput. Phys.*, 103:16–42.

Meneveau, C., Lund, T. S., and Cabot, W. (1996). A lagrangian dynamic subgrid-scale model of turbulence. *J. Fluid Mech.*, pages 353–386.

Nguyen, P. D. and Bruel, P. (2003a). Turbulent reacting flow in a dump combustor: experimental determination of the influence of the inlet equivalence ratio difference on the contribution of the coherent and stochastic motions to the velocity field dynamics. In *Paper 2003-0958, 41st Aerospace Sciences Meeting and Exhibit, Reno, USA, January 2003*. AIAA.

Nguyen, P. D. and Bruel, P. (2003b). Turbulent reacting flow in a dump combustor: some specific aspects related to the modelling of turbulent transports. In *19th ICDERS, Hakone, Japan*. ISBN 4-9901744-0-1/-2.

Pitsch, H. and de Lageneste, L. D. (2002). Large-eddy simulation of premixed turbulent combustion using a level-set approach. *Proc. Comb. Inst.*, 29:2001–2008.

Poinsot, T. and Lele, S. K. (1992). Boundary conditions for direct simulations of compressible viscous flows. *J. Comput. Phys.*, 1(101):104–129.

Poinsot, T. and Veynante, D. (2005). *Theoretical and Numerical Combustion*. R. T. Edwards, Inc.

Renou, B. and Boukhalfa, M. (2003). Experimental analysis of a premixed turbulent v-flame. *Private communitation*, INSA de Rouen and CNRS-CORIA.

Roux, S., Lartigue, G., Poinsot, T., Meier, U., and Berat, C. (2005). Studies of mean and unsteady flow in a swirled combustor using experiments, acoustic analysis, and large eddy simulations. *Combust. Flame*, In press, Available online 3 February 2005.

van Oijen, J. A., Lammers, F. A., and de Goey, L. P. H. (2001). Modeling of complex premixed burner systems by using flamelet-generated manifolds. *Combust. Flame*, 127(3):2124–2134.

Vervisch, L., Hauguel, R., Domingo, P., and Rullaud, M. (2004). Three facets of turbulent combustion modelling: Dns of premixed v-flame, les of lifted nonpremixed flame and rans of jet-flame. *J. of Turbulence*, 5(4):1–36.

Veynante, D. and Poinsot, T. (1997). Effects of pressure gradients on turbulent premixed flames. *J. Fluid Mech.*, 353:83–114.

Veynante, D., Trouvé, A., Bray, K., and Mantel, T. (1997). Gradient and counter-gradient scalar transport in turbulent premixed flames. *J. Fluid Mech.*, 332:263–293.